International Journal of GEOMATE, July., 2021, Vol.21, Issue 83, pp.43-49
ISSN: 2186-2982 (P), 2186-2990 (O), Japan, DOI: https://doi.org/10.21660/2021.83.Gx325
Geotechnique, Construction Materials and Environment

STUDY OF THE INFLUENCE OF BACKFILLING ON STABILITY AND LOCATION OF REMAINING STOPES IN SILL PILLAR RECOVERY

Huawei Xu, and Derek B. Apel*

Faculty of Engineering, University of Alberta, Canada

*Corresponding Author, Received: 11 May 2020, Revised: 23 Jun. 2020, Accepted: 15 Jul. 2020

ABSTRACT: To extract steeply dipping orebodies, many mines in Canada have adopted the sublevel stoping method, such as blasthole stoping (BHS) and sublevel longhole retreat (SLR). In such methods, sill pillars are initially kept in place to support the weight of the overburden in underground mining. After the stope mining is complete, the stope voids will be backfilled with cemented rockfill (CRF). The strength of the CRF affects the stability of the adjacent stopes in the sill pillar recovery excavation scheme. Sill pillar recovery may cause prolonged failure, fatality, and equipment loss. Choosing a rational location of the last mined stope in sill pillar recovery can effectively eliminate the possible instability caused by the sill pillar recovery process. This paper uses the Finite Element Method (FEM) to present a comparison of sidewall swellings, floor heaves, and the roof subsidence of the crossing cuts in each stope among different last mined stope location scenarios. At all the 21 location scenarios, most of the roof corner displacements in undercuts are less than 10 cm, while in the overcuts, all the displacements in roof corners are over 10 cm. The values of the floor heave in the overcuts are more than 7 times that in the undercuts. Roofs in both undercuts and overcuts are prone to failures. Floors in the undercuts are more stable than the floors in the overcuts. For the optimum location of the last mined stope in sill pillar recovery, the last mined stope should be at least four-stope-width away from the two sill pillar edges.

Keywords: Sill pillar recovery, Crossing cuts, Cemented rockfill, Unmined stopes, Stope location

1. INTRODUCTION

Pillar recovery is the practice of forming a series of pillars and then partially or totally extracting some or all of the pillars [1]. Pillar recovery is considered the most hazardous form of underground mining and is thought to be an art as much as a science [2]. Sill pillars are initially left in place to support the great weight of the overburden in underground mining. Pillar recovery is an important step in mining operations, specifically in the area of maximizing resource recovery. During the process of pillar recovery, it is possible to induce risks, such as overlaying rock subsidence, stope failure and pillar failure. Researchers initiated and proposed empirical, analytical theories and numerical technical methods to assess the stability and guarantee the safety of miners and mining equipment. Hudyma and Potvin studied microseismic, conventional ground control instruments, numerical modelling, and visual observations to understand the mechanisms of pillar failures [3,4]. Mark [1] and Iannacchione [5] analyzed the strengths and weaknesses of MHRA techniques and assessed the major hazard risks to evaluate sill pillar recovery in two room-and-pillar mines. Zhukova used monitored underground seismic registrations and mathematical models to improve the safety operations in pillar recovery [6]. Langston designed the stope layout, extraction procedure, and ground support, which were applied to successfully recover a pillar [7]. Ghasemi assessed the risk of pillar recovery operations and classified that risk into four categories by using indicators [8,9]. Beruar developed proper stope sequencing to avoid the highly stressed area during pillar recovery [10]. Valley optimized the mining sequence and suggested new directions for the different methods and the potential shortcomings [11]. Townend proposed five mitigation strategies to mitigate the high-stress concentration while mining sill pillars [12].

Sill pillar recovery in the blasthole stoping (BHS) mining method, has not been widely discussed. BHS mining includes two sublevels. The one at the top of the stope is for drilling (overcut), and the other at the bottom is for production (undercut). For most hard rock mines in Canada, orebody blocks are usually steeply inclined, and the BHS method is widely used.

2. RESEARCH SIGNIFICANCE

In underground mining, in order to improve the production, several mining levels are active in the mining process at different mining depths, simultaneously. The mining process will cause the redistributed stresses, and the redistributed stress could make transfers horizontally and vertically. The transferred stress may contribute to failures of the stopes and damages to the mining equipment. For the sake of the safety of the mining zones, sill pillars are commonly reserved to prevent the vertical transfer of the redistributed stress, especially in the steeply dipping orebodies. Using the CRF to backfill the mined voids provides an effective way to recover the reserved sill pillars.

The reserved sill pillar consists of several mining stopes, and each stope can contain thousands of tons of materials. Compared with the backfilled CRF in the mined voids, the unmined stopes in the sill pillar will provide more support than the backfilled CRF. Recovering the unmined stopes in the sill pillar may cause the failure of the unmined stopes, especially for the last one or two stopes. Then, deciding the location of the last mined stope in the sill pillar plays a key role in recovery the whole sill pillar, and this paper studies the location of the last mined stope.

3. BACKGROUND

The hard rock mine in this paper applies the blasthole stoping (BHS) mining method. In this method, the overcut is first excavated from the top of the stope and the undercut is excavated from the bottom of the stope. In general, overcuts and undercuts have the same intersections and sizes. Once the overcuts and the undercuts are excavated, the blastholes are drilled from the overcuts down to the undercuts. When the blastholes are loaded with explosives and blasted, the fragmented ore drops down to the earlier prepared undercuts. Then fragmented ore is picked up by the scoop trams and is transported to the ground surface. After the ore is removed from the stope, the low-profile concrete trucks dump the CRF material from the overcut down to the open stope voids. Once the CRF material sets, the neighboring stopes can be mined [13].

The strength of the backfilled cemented rockfill (CRF) affects the displacement/subsidence of the open pit benches which determines the stability of the whole mine site, especially for the mines transferred from open pit mining to underground mining. Lingga conducted laboratory experiments to determine the ratios among the aggregates, cement, and water to achieve a better ratio and higher strength of the backfilled cemented rockfill (CRF), considering the cost of the materials [14]. Sepehri predicted the stress redistribution caused by the excavation and the ground subsidence with the influence of the redistributed stress and the backfilled cemented rockfill (CRF) [15,16]. Concretes, usually mixed with the by-product materials, are also widely used in the backfilling mining method. The strength of the concrete is a key factor when use the concrete to backfill the mined stope voids. In order to determine the strength of concrete, an Artificial Neural Network (ANN) was applied to establish the relationship between the various input parameters and the compressive strength of normal concrete and High-Performance Concrete (HPC) [17]. In order to reduce the cost of the concrete production, laboratory tests were conducted to replace some percent of cement in the concrete with the by-product materials of power plant without reducing the strength of the concrete [18]. Studying the structures of concrete gives a better understanding of how the concrete works. Kropacek studied the interaction between the concrete structure and the subsoil and presented the experiments that showed the concrete mixed with steel fibers had a positive effect on reducing volume changes at the early stages of setting and hardening process [19].

For the recovery of sill pillars, most current research focuses on the room-and-pillar mining method. In these studies, the stress movement was mainly triggered by the layers above the mining level. Most of the studies did not take backfilling into account. The relationship between the influence of the backfilled CRF and the stress redistribution and ground displacement in the process of sill pillar recovery has not been widely discussed.

Sill pillars play a key role in maintaining the safety of the mining area above their location and below it. They can prevent mining-induced stresses from moving from one block to another. Recovering the sill pillar safely can make the most use of the minerals. However, recovery of the reserved sill pillar can also trigger catastrophic problems. Then the stope sequences in the sill pillar recovery become significant. When the backfilled CRF is involved, the rational location of the last mined stope in the recovery process also becomes more significant.

4. ESTABLISHING THE NUMERICAL MODELLING

Numerical modeling plays an important role in the assessment and designation of engineering projects in rock mass [20–24]. Numerical simulation implements the advantage of predicting possible failures in the way of identifying the observed failure mechanism. FEM is one of the widely used numerical methodologies in engineering because of its flexibility in solving material heterogeneity, non-linearity. As a well-developed and verified commercial code software, Abaqus is capable to handle numerical models with material complexity, complicated boundary conditions, and dynamic problems, and it is also user-friendly [25]. Since the acceptable constitutive model failure criteria in Abaqus for rock is the Mohr-Coulomb failure criteria [26], so both the 2D and 3D models use the Mohr-Coulomb failure criteria for the simulation calculation.

4.1 Creating The FE Model

The hard rock mine in this paper was initially operated as an open-pit mine. Once the open-pit mining was completed, the operation shifted to underground mining. Under the open pit, it is the underground mining zone: MZ#1. The dimensions of the full-size FE model are 1200×1200×700 m (length×width×depth), as shown in the following Fig.1.

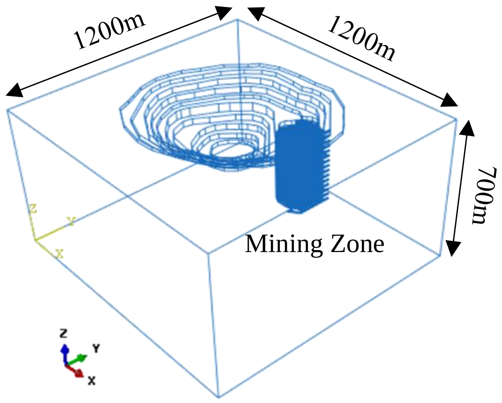

Fig.1 Full-size FE model of mine

The analysis of the mining-induced and backfilling-induced stress field during the sill pillar recovery in this paper is global to local. First, we created a 3D numerical model, as shown in Fig.1. To achieve better results of the redistributed stress field, in this full-size model, the ten-node quadratic tetrahedron mesh element (C3D10) was used to conduct the simulation. Next, the mining-induced redistributed stress field of the researched sill pillar was extracted from the full-size 3D model and applied to the simplified 2D sill pillar model. In the simplified 2D model, the four-node bilinear plane quadrilateral mesh element (CPE4R) was used [26].

The modelled mining pipe has, as shown in Fig. 2, seven mining levels. The sill pillar located in the middle of the mining pipe in MZ#1. The mining depth of sill pillar is 270 m from the ground surface. The sill pillar is 25m high and contains twenty-one mining stopes. The heights of the stopes in each level and sill pillar are the same, which are 25 m, and the width is 7 m. As for the overcuts and undercuts in the stope in the sill pillar, the height is 5m, and the width is the same as that of the stope, and it is 7m. The sill pillar is located between level N1504 and level N1505, as shown in the following Fig.2.

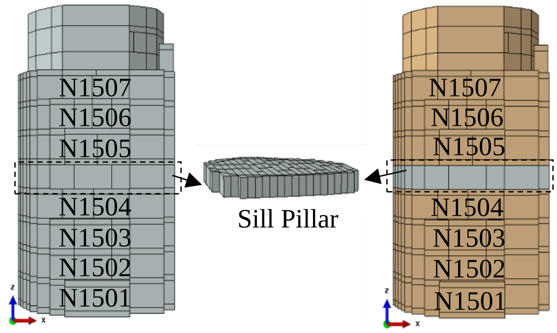

Fig.2 Modelled pipe and sill pillar

4.2 Mechanical Properties Of The Modelled Rock And Backfilling CRF

Table 1 shows the rock mechanical properties applied in the model in this study [15,16,27]. Here, E is the elastic Young's modulus, ν is the Poisson's ratio, γ is the unit weight, ϕ is the angle of friction, C is the cohesive strength, σ_c is the uniaxial compressive strength and σ_t is the tensile strength.

Table 1 Material properties

Materials	E (GPa)	ν	γ (MN/m^3)	ϕ (°)	C (MPa)	σ_c (MPa)	σ_t (MPa)
MZ#1	18.7	0.26	0.024	26.4	4.2	66	3.4
Granite	24	0.3	0.026	45	9.3	130	0
CRF	2	0.3	0.022	35	1.2	1.5	0

Figure 3 shows the three examples of stope locations in the sill pillar. The simplified 2D model has a size of 100×147 m (height×width). Above the sill pillar, it is 25 m thick backfilled CRF, and below the sill pillar, it is 50 m thick backfilled CRF.

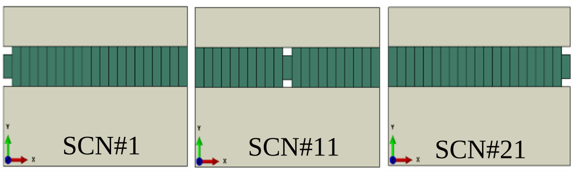

Fig.3 Example stope location layout of sill pillar

SCN#1 means that the last mined stope is at the left edge of the sill pillar. SCN#11 means the last mined stope is in the middle of the sill pillar. SCN#21 means the last mined stope is at the right edge of the sill pillar. During the simulation process, the location of the last mined stope changes from SCN#1 to SCN#21. The upper void areas in the figure are the overcuts in the stopes, and the lower void areas in the figure are the undercuts in the stopes. The color of dark green represents the kimberlite orebody in the sill pillar, and the color of white represents the backfilled CRF, as shown in Fig. 3.

5. RESULTS AND DISCUSSION

In underground mining engineering, the rectangular intersections of undercuts and overcuts are commonly used. Due to the high ground stress and the mining-induced redistributed stress, the corners in the roofs and floors of the undercuts and overcuts in the stopes can easily generate the stress concentration. The excavation of the undercuts and overcuts cause stress release on the free surface of roof, floor, and sidewall, which will cause roof displacement, floor heave and sidewall swellings.

Monitoring and measuring the displacement at different locations in the undercuts and overcuts are crucial to detect the possible and potential failures in the free surfaces of roof, floor, and sidewall, and improve the safety of the undercuts and overcuts in the process of mining and transportation.

In order to better measure and compare the displacements of different locations in the undercuts and overcuts in the sill pillar among different stope location scenarios during the simulation process, eight locations are numbered in the undercuts and overcuts. The stability of these locations is an external indicator of the overcuts and undercuts in the stopes.

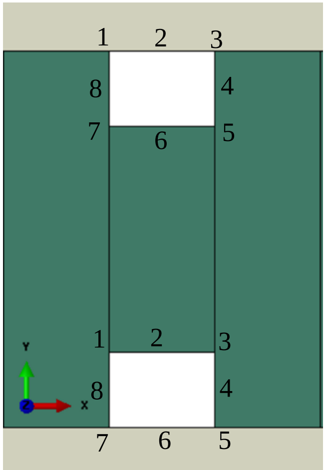

Fig.4 Numbered locations for comparison

As shown in above Fig.4, in both undercut and overcut, Node 1 and Node 3 are the two top roof corners, while Node 2 and Node 6 locate in the middle of the roof and floor, respectively. Node 4 and Node 8 are in the middle of sidewalls, and Node 5 and Node 7 are the two floor corners.

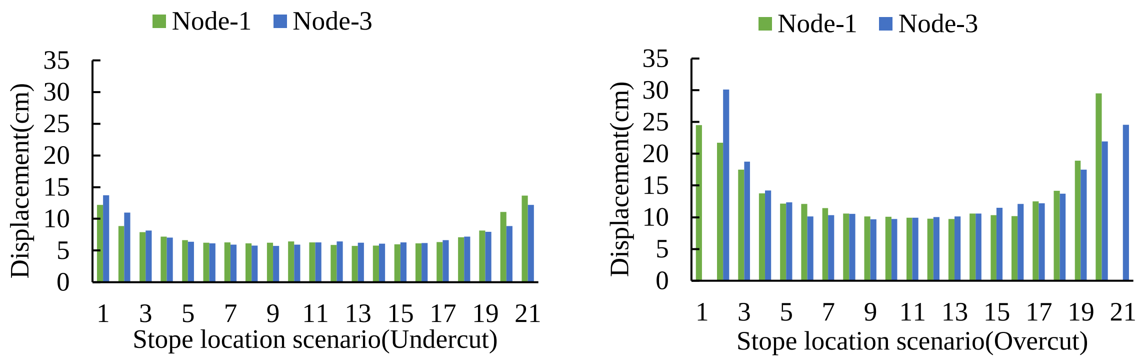

Fig.5 Displacement at Node-1& Node-3 in both undercut and overcut

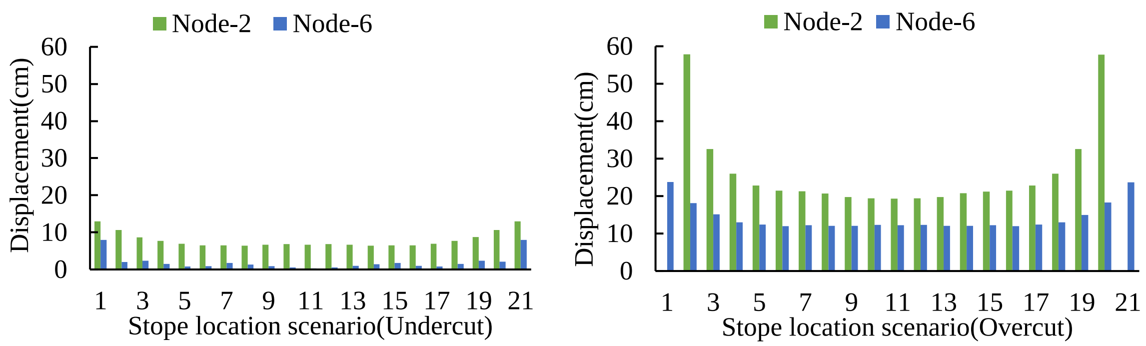

Fig.6 Displacement at Node-2 & Node-6 in both undercut and overcut

As shown in the above Fig.5, compared with the displacement of the roof corners in the overcuts, the displacement in the undercuts is much smaller. For the undercut, expect for the locations far from the sill pillar center, there is almost no difference between different stope location scenarios. For most of the displacements, at the same location number, the overcut is about two times of that of the undercut. At each location scenario, the two roof corners have almost the same displacement. There is a significant possibility that the roof corners in the overcuts will fail at the two edges of the sill pillar if the last mined stopes are located at the two edges of the sill pillar.

Figure 6 shows the roof displacement and floor heave in both the undercut and overcut. Unlike the roof corners displacement in Fig.5, the roof displacement in both the undercut and overcut is larger than the floor heave. Similar to the roof corners, the roof displacement and floor heave in the overcut are much larger than those in the undercut. In the undercut, there is almost no floor heave, and the roof displacement is negligible. The roof displacement in the overcut shows a slight difference except for the two edge location scenarios, while for the floor heave in the overcut, the edge location scenarios are almost the same at various locations. For the sake of safety, more supports should be installed in the roof and floor in the overcut.

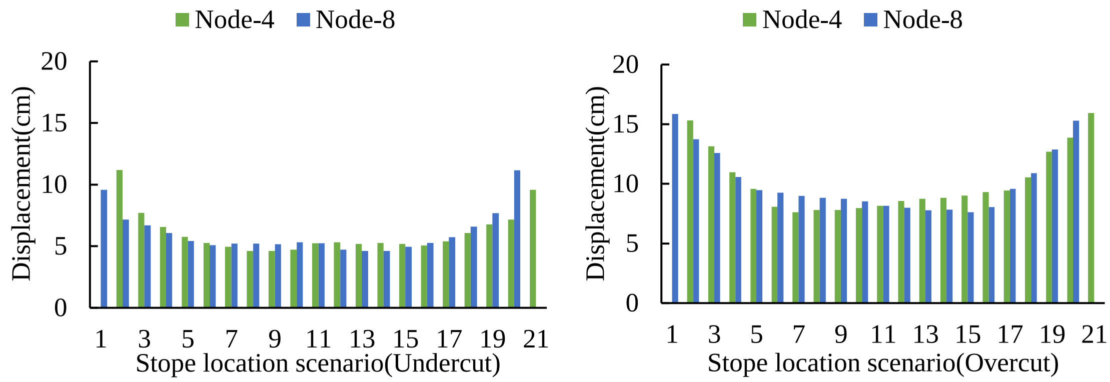

Fig.7 Displacement at Node-4 & Node-8 in both undercut and overcut

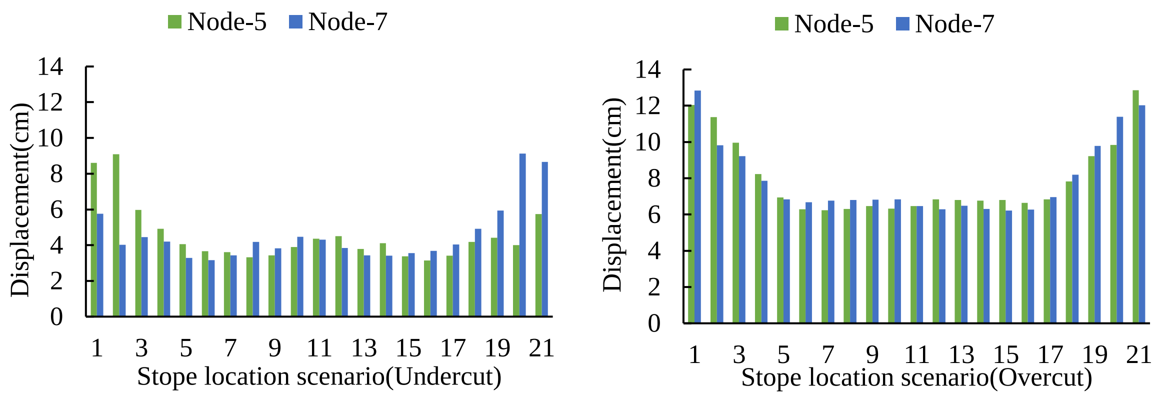

Fig.8 Displacement at Node-5 & Node-7 in both undercut and overcut

Figure 7 shows the configuration of the sidewall swellings. The swellings show a gradual changing trend from the edges of the sill pillar to the center of the sill pillar. In the undercut, the sidewall swellings are almost the same at the same stope location scenarios, and the swellings are considerably lower, most of the swellings are around 5 cm. The sidewall swellings in the overcut are almost twice the size of those in the undercut at the same stope location scenarios, and most of the swellings are around 10 cm. At the edges, the swelling is around 15 cm in overcut. More attention should be paid to the safety of the sidewalls in the overcuts.

Floor heave is an important indicator of roadway safety in mining engineering. Figure 8 shows the heave of the two floor corners. The heave of the two floor corners at the same stope location in the sill pillar is almost the same. Most of the heaves are less than 10 cm for the undercut. For the overcut, the floor corners are in the granite; and for the undercut, the floor corners are in the backfilled CRF. The floor corner heave in the overcut is much larger than that in the undercut, which means the sill pillar takes most of the redistributed stresses and plays a key role in maintaining the safety in the mining process both above and underneath the blocks.

6. CONCLUSIONS

From the roof displacements, floor heaves, and sidewall swellings in both undercuts and overcuts, the sill pillar in this hard rock mine plays a key role in maintaining the safety of the mine throughout the mining and backfilling processes.

In the same stope location scenario, compared with overcut, the displacement of the roof corners in an undercut is smaller, and most of the roof corner displacements in undercuts are less than 10 cm, while in the overcuts, all the displacements in roof corners are over 10 cm. At the three location scenarios of each edge of the sill pillar, the displacements are over 15 cm, and the maximum value can be around 30cm. From the view of the roof corner displacement in undercuts and overcuts, the roof in the undercut is more stable than that in the overcut, and more protective measures should be taken in the roof of the overcut.

The floor heave in the undercut is tiny, and most of them are under 3 cm. The floor heave in the overcuts are more than 7 times of that in the undercuts, which means the floors in the undercuts are more stable than the floors in the overcuts. Also, the roof displacements in the overcuts are more than 2 times that in the undercuts, and all the roof displacements are over 20 cm in the overcuts. The sidewall swellings in the undercuts are about half of that in the overcuts at the same location scenarios.

Roofs in the overcuts and floors in the undercuts are the backfilled CRF. The strength of the CRF is lower than the sill pillar hard rock, then the roof displacement in overcuts is much larger than that in undercuts. In both undercuts and overcuts, more attention should be paid to the supports on the roof than on the floor.

Based on the above conclusions, for the optimum location of the last mined stope in sill pillar recovery, the last mined stope can be any location between No.5 to No.17 in the sill pillar, and the last mined stope location should avoid the edge of the sill pillar.

In general, in order to recover the maximum amount of the sill pillar and improve the safety of the recovery process, in the process of sill pillar recovery, especially in the backfilling mining method, the last mined stope location should avoid the edge of the sill pillar and keep several stope-width from the sill pillar edge.

7. ACKNOWLEDGEMENTS

This study was supported by the Natural Sciences and Engineering Research Council of Canada (NSERC) under the Collaborative Research and Development (CRD) Grant (NSERC RGPIN-2019-04572). The supports from China Scholarship Council were acknowledged. The supports from WestGrid and Compute/Calcul Canada were gratefully acknowledged.

8. REFERENCE

[1] Mark C., Chase F., and Pappas D., “Reducing the Risk of Ground Falls During Pillar Recovery,” Trans Soc Min Eng, 2003, pp. 153–160.

[2] Christopher M. and Michael G., “Preventing Roof Fall Fatalities During Pillar Recovery : A Ground Control Success Story,” Int. J. Min. Sci. Technol., vol. 27, no. 1, 2017, pp. 107–113.

[3] Hudyma M. R. and Mining B., “Geomechanics of Sill Pillar Mining,” in Proceeding of the 1st North American Rock Mechanics Symposium, 1994, pp. 969–976.

[4] Potvin Y. and Hudyma M. R., “Open Stope Mining in Canada,” in Proceedings of the MassMin2000, Brisbane., 2000, no. January 2000.

[5] Iannacchione A. T., “Major Hazard Risk Assessment Applied to Pillar Recovery Operations,” In: Proceedings of the 28th international conference on ground control in mining. Morgantown, West Virginia University, USA; 2009, 2009, pp. 261–270.

[6] Zhukova S., Korchak P., Streshnev A., and Salnikov I., “Geodynamic Rock Condition , Mine Workings Stabilization During Pillar Recovery at the Level + 320 m of the Yukspor Deposit of the Khibiny Massif,” in VII International Scientific Conference “Problems of Complex Development of Georesources,” 2018, vol. 02022.

[7] Langston R. B., Kirsten H. A. D., Niemi E. A., and Marjerison J. A., “Extraction of a Remnant Sill Pillar Under Challenging Ground Conditions at the Stillwater Mine , Nye , Mt .,” 2006.

[8] Ghasemi E., Shahriar K., and Sharifzadeh M., “A New Method for Risk Assessment of Pillar Recovery Operation,” Saf. Sci., vol. 48, no. 10, 2010, pp. 1304–1312.

[9] Ghasemi E., Ataei M., Shahriar K., Sereshki F., and Esmaeil S., “Assessment of Roof Fall Risk During Retreat Mining in Room and Pillar Coal Mines,” Int. J. Rock Mech. Min. Sci., vol. 54, 2012, pp. 80–89.

[10] Beruar O., Forsythe A. S., and Yao M., “Sill Pillar Mining in the Main Orebody at Vale ’ s Coleman Mine,” in 45th US Rock Mechanics / Geomechanics Symposium, vol. 9300, no. 3830 L, 2011, pp. 1–7.

[11] Valley B., Pun W., Hutchinson D. J., and Madjdabadi B., “Rock Mass Change Monitoring in a Sill Pillar at Vale ’ s Coleman Mine (Sudbury , Canada),” in Canadian RM Conference, 2012, no. January.

[12] Townend S. and Sampson-Forsythe A., “Mitigation Strategies for Mining in High Stress Sill Pillars at Coleman Mine – A Case Study,” Aust. Cent. Geomech., 2014, pp. 65–78.

[13] Darling P., Mining Engineering Handbook, Third. Society for Mining, Metallury, and Exploration, 2011.

[14] Lingga B. A., “Investigation of Cemented Rockfill Properties Used at a Canadian

Diamond Mine," University of Alberta, 2018.
[15] Sepehri M., "Finite Element Analysis Model for Determination of In-situ and Mining Induced Stresses as a Function of Two Different Mining Methods Used at Diavik Diamond Mine," University of Alberta, 2016.
[16] Sepehri M., Apel D. B., and Hall R. A., "Prediction of mining-induced surface subsidence and ground movements at a Canadian diamond mine using an elastoplastic finite element model," Int. J. Rock Mech. Min. Sci., vol. 100, no. October, 2017, pp. 73–82.
[17] Nguyen T. T., Ngoc L. T., Vu H. H., and Thanh T. P., "Machine Learning-Based Model for Predicting Concrete Compressive Strength," Int. J. GEOMATE, vol. 20, 2010, no. 77, pp. 197–204.
[18] Rodvinij P. and Ratchakrom C., "Effect of Cement Replacement By Fly Ash and Fgd Gypsum on Strength of Subbase," Int. J. GEOMATE, vol. 20, no. 80, 2021, pp. 9–16.
[19] Kropacek M., Mynarcik P., Cajka R., "Concrete Structures Interacting with Subsoil," Int. J. GEOMATE, vol. 18, no. 69, 2020, pp. 136–142.
[20] Jing L. and Hudson J. A., "Numerical methods in rock mechanics," Int. J. Rock Mech. Min. Sci., vol. 39, no. 4, 2002, pp. 409–427.
[21] Jing L., "A review of techniques, advances and outstanding issues in numerical modelling for rock mechanics and rock engineering," Int. J. Rock Mech. Min. Sci., vol. 40, no. 3, 2003, pp. 283–353.
[22] Hart R., "Enhancing rock stress understanding through numerical analysis," Int. J. Rock Mech. Min. Sci., vol. 40, no. 7–8, 2003, pp. 1089–1097.
[23] Wiles T. D., "Reliability of numerical modelling predictions," Int. J. Rock Mech. Min. Sci., vol. 43, no. 3, 2006, pp. 454–472.
[24] Cai M., "Influence of stress path on tunnel excavation response - Numerical tool selection and modeling strategy," Tunn. Undergr. Sp. Technol., vol. 23, no. 6, 2008, pp. 618–628.
[25] Sun Y., Chen Y., and Wang Z., "Numerical simulation of inner support for excavation based on FEM software ABAQUS," Appl. Mech. Mater., vol. 236–237, 2012, pp. 632–635.
[26] Dassault Systèmes Simulia Corp., "Analysis User's Manual Volume 1: Introduction, Spatial modeling, execution and output," Abaqus 6.12, vol. I, 2012.
[27] Xu H. W. and Apel D. B., "Optimum location of last-mined stope with the influence of backfilling," J. Sustain. Min., vol. 19, no. 4, 2020, pp. 212–220.